



**Investigation of Stainless Steel Pickling Liquor as a
Precursor for High Capacity Battery Electrode Materials**

Journal:	<i>RSC Advances</i>
Manuscript ID:	RA-ART-09-2014-011539.R1
Article Type:	Paper
Date Submitted by the Author:	22-Oct-2014
Complete List of Authors:	Sanghvi, Sheel; Rutgers University, Energy Storage Research Group Pereira, Nathalie; Rutgers University, Energy Storage Research Group Halajko, Anna; Rutgers University, Energy Storage Research Group Amatucci, Glenn; Rutgers University, Energy Storage Research Group

Investigation of Stainless Steel Pickling Liquor as a Precursor for High Capacity Battery Electrode Materials

Sheel Sanghvi, Nathalie Pereira, Anna Halajko, Glenn G. Amatucci
Energy Storage Research Group
Dept. of Materials and Engineering, Rutgers University
North Brunswick, New Jersey 08902

Abstract

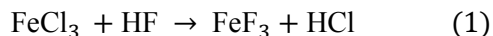
Stainless steel and battery manufacturing industries can be brought together for mutual economic and environmental benefits by utilizing post process stainless steel pickling liquor waste as precursor for high energy iron fluoride based positive electrode materials in batteries. This study analyzes the feasibility, the environmental, and economic cost of the ferric fluoride (FeF_3) synthesis approach through the use of recycled pickling liquor from the stainless steel fabrication industry. This new synthesis method is determined as more environmentally friendly than the current methods of disposing of spent stainless steel pickling liquor and producing ferric fluoride. X-ray diffraction analysis demonstrated the synthesis occurs in two steps: the conversion of spent pickling liquor to produce the crystalhydrate $\beta\text{-FeF}_3 \cdot 3\text{H}_2\text{O}$ followed by its dehydration into anhydrous FeF_3 . Materials obtained from pickling solutions were found electrochemically active with improved cycling stability and similar capacity compared to commercial FeF_3 . Pickling solutions synthesized with nickel and chromium to better replicate spent pickling waste showed best cycling stability.

Introduction

Transportable power sources are enabling technologies for an enormous breadth of devices that bring significant benefit to society. Although almost all applications require high performance, the sheer scale of battery production demands appropriate environmental responsibility and economic feasibility.

Metal fluoride nanocomposites have been shown as an appealing approach to positive electrode materials for primary and secondary batteries based on their high energy densities compared to the current state of the art. (1) More specifically, iron-based materials are desirable based on iron's low toxicity, abundance and therefore potential lower cost. However, the fluoride component can contribute a fairly significant processing cost and possible impact to the environment especially if processed in a non responsible manner.

The most common process of producing FeF_3 is shown by the reaction in Equation 1. A constant stream of anhydrous hydrogen fluoride (HF) is passed over anhydrous ferric chloride (FeCl_3) in a heated, oxygen-free reactor. (2)



Such method of production of iron fluorides poses a significant environmental issue through an unnecessary, extra exploitation of energy and precursor materials.

A possible alternative to produce FeF_3 is to utilize pickling liquor, a waste product of the stainless steel industry. The stainless steel manufacturing industry requires a final process known as pickling to etch the

surface of as processed stainless steel and restore the protective effects of chromium and other surface oxides. After the pickling process is completed, the acid is rinsed off the surface of the steel and stored in waste containers as spent pickling liquor (SPL). As discussed in detail below, such SPL typically contains nitric acid, hydrofluoric acid, iron and various other metals.

Large amounts of spent liquor need to be disposed of each year by stainless steel manufacturers leading to a non insignificant cost to the product. Although some stainless steel manufacturers attempt to regenerate the acids or recover the metals from the spent liquor, most processes are not fully effective leading to appreciable environmental and financial costs. A frequently employed method to treat spent liquor is through lime neutralization.

Both processes of producing new FeF_3 and disposing spent liquor introduce certain environmental impacts. A quantitative metric needs to be enacted to compare if the impact of these process outweigh the impact of producing FeF_3 from SPL. This is accomplished through use of the Waste Reduction Algorithm (WAR) GUI created by the United States Environmental Protection Agency. The WAR GUI produces a numerical score for a chemical process called the potential environmental impact (PEI) to describe the impact a process will have. This is defined in further detail below.

The PEI values obtained from the WAR GUI for each of the processes will be plugged into Equation 2 to estimate the environmental impact of the fabrication of the FeF_3 from the spent liquor compared to the combination of the spent liquor disposal and the current commercial FeF_3 fabrication process. Appropriate satisfaction of this equation would justify the environmental benefit of converting spent pickling liquor into FeF_3 .

$$\text{Env. Impact}_{\text{New FeF}_3} + \text{Env. Impact}_{\text{SPL Disposal}} > \text{Env. Impact}_{\text{FeF}_3 \text{ from SPL}} \quad (2)$$

However, before any environmental calculations can be completed, a chemical pathway behind the conversion process must be demonstrated. A possible pathway to convert SPL into iron fluorides is the precipitation of $\beta\text{-FeF}_3 \cdot 3\text{H}_2\text{O}$ from SPL followed by dehydration into FeF_3 . Other research groups have independently studied different points of this pathway. Tjus et al. and Sartor et al. confirm that $\beta\text{-FeF}_3 \cdot 3\text{H}_2\text{O}$ crystals can be separated from spent liquor. (3) (4) Quite recently, Myung et al. and Liu et al. produced the anhydrous form of ferric fluoride from the crystal hydrate. (5) (6) . This paper aims to unite all points to form one complete method of an environmentally sound supply stream to show that the waste pickling liquor from the stainless steel industry can be transformed to high value added component product of high energy density iron fluoride for battery applications. This study also encompasses the evaluation of the electrochemical activity of the products synthesized from pickling liquors with a comparison to a commercial FeF_3 material.

Experimental

Sample solutions of spent pickling liquor were synthesized by dissolving iron nitrate hydrate $\text{Fe}(\text{NO}_3)_3 \cdot 9\text{H}_2\text{O}$ (Alfa Aesar), chromium nitrate hydrate $\text{Cr}(\text{NO}_3)_3 \cdot 9\text{H}_2\text{O}$ (Sigma Aldrich), and/or nickel nitrate hydrate $\text{Ni}(\text{NO}_3)_2 \cdot 6\text{H}_2\text{O}$ (Sigma Aldrich) in a solution of hydrofluoric acid (HF) (48%, Sigma Aldrich) and deionized water. Solutions were stored at room temperature for one week to allow for crystallization to fully occur. The produced crystals were first filtered with filter paper (Whatman 542)

then washed with three 10mL aliquots of ethanol (Sigma Aldrich). Finally, the water adhering to the surface of the crystals was removed by drying overnight at 70°C in air with <1% relative humidity.

The dehydration of the crystals was completed in a Lindberg/Blue-M tube furnace at 150°C-400°C under flowing argon for various intervals of time. Additionally, differential scanning calorimetry (TA-Instruments Q10) was performed using pans hermetically sealed in a helium environment subsequently heated at a rate of 5°C/min from room temperature to 450°C. X-ray diffraction was completed using a Bruker D8 Advance diffractometer with a 0.02° 2 θ step size, a 1.9 sec/step count, and a 15-60° 2 θ angle span and a CuK α x-ray source. Furthermore, using the software TOPAS, x-ray diffraction patterns were fitted by Rietveld Refinement to estimate crystal size. Scanning Electron Microscopy was performed on a Zeiss Sigma Field Emission SEM with an Oxford INCA PentaFETx3 Energy Dispersive Spectroscopy (EDS) attachment. The secondary electron detector was used with a voltage of 5.00 kV and a working distance of 7.9 millimeters.

In order to evaluate the electrochemical performance of the materials obtained from pickling liquor and compare to commercial FeF₃ (Advanced Research Chemicals), nanocomposites were fabricated by high-energy mechanomilling. (7) The iron fluorides either synthesized from pickling liquor or obtained from a commercial source were milled with 15wt% activated carbon (ASupra, Norit) for 1h in helium.

Electrode tapes were fabricated according to the Bellcore developed process. (8) The active materials were mixed in acetone (Aldrich) with poly(vinylidene fluoride-co-hexafluoropropylene) binder (Kynar 2801, Elf Atochem), carbon black additive (Super P, MMM) and dibutyl phthalate plasticizer (Aldrich). After plasticizer extraction in anhydrous ether (Aldrich), the electrodes typically consisted of 57.25% active material, 12% carbon additive, and 31% binder. Two-electrode coin cells were assembled using a lithium foil counter electrode and glass fiber separators (GF/D, Whatman) saturated with 1M LiPF₆ in ethylene carbonate:dimethyl carbonate electrolyte (50:50 in vol.%) from BASF. The cells were cycled at 60°C under a constant current of 7.5mA/g based on the weight of the nanocomposite, between 1.5 and 4.5V.

Various sources of information were consulted to determine the material flow and energy consumption for each production stream. Using such data, an environmental impact estimate was calculated using the WAR GUI software to generate a PEI score. The PEI is composed of a sum of eight categories: Human Toxicity Potential by Ingestion, Human Toxicity Potential by Dermal Contact or Inhalation, Aquatic Toxicity Potential, Terrestrial Toxicity Potential, Global Warming Potential, Ozone Depletion Potential, Photochemical Oxidation Potential, and Acidification Potential. Each category is assigned a specific weight depending on how important that environmental concern is to the chemical process. For this study, all categories were assumed to have equal weight. Furthermore, for each of the eight categories, each chemical is assigned a normalized value which is computed from toxicology information in the program's database and literature. The normalized values are added together to create the PEI. The specific PEI of interest for this paper is calculated as a summation of the impact of chemicals produced and energy consumed.

Many assumptions are considered for all PEI calculations in this study. For example, the crystals produced from SPL by the process described later in this paper are assumed to be composed primarily of FeF₃ with nominal amounts of CrF₃. Additionally, except for the SPL composition, if the amount of

reactants or products in a specific chemical process is given as a range of values, then the smallest amounts of each reactant or product are used for calculations. This will minimize the environmental impact of the chemical process and provide the best case scenario. Another assumption is that non-descriptive items such as solid waste or heavy metals are not included in PEI calculations, which causes the mass balance to be slightly off. Also, the impact of transportation between facilities was not included in PEI calculations because of the multiple options and distances for production facilities. Next, the energy impact was combined to include all utilities such as heating, electricity, refrigeration, etc. and gas was assumed to be the only source to generate the energy. This provides a uniform basis for energy calculations. Finally, the impact of process water was ignored because water has an insignificant impact and can be used in varying quantities for different processes.

Results

1. Disposal process of spent pickling liquor from the stainless steel industry

Spent liquor typically has the composition of the “Industrial SPL” shown in Table 1. The spent liquor is disposed of by lime neutralization. Calcium hydroxide or slaked lime is introduced into a tank containing the liquor to raise the pH of the solution and precipitate ferric hydroxide and calcium fluoride. The solid waste from this reaction is removed by filtering and then, it is pressed dry and landfilled. The aqueous waste, which contains calcium and nitrate ions, is either released into a stream or sent to a wastewater treatment plant for further processing. Figure 1 shows the inputs and outputs of this process.

2. Current commercial synthesis process of FeF_3

Anhydrous ferric fluoride is rarely fabricated at industrial levels because the hydrated, chloride form of the metal salt is preferred. However, it is possible to manufacture anhydrous ferric fluoride by passing a stream of anhydrous hydrogen fluoride over anhydrous ferric chloride in an oxygen-free environment. (9) Figure 2 below shows this process along with the production of the precursors.

The precursors for ferric fluoride production are hydrogen fluoride and ferric chloride. Hydrogen fluoride is synthesized by reacting concentrated sulfuric acid with the mineral fluorspar in a heated reactor. (10) It is then dehydrated by condensation and distillation. A co-product of this reaction is calcium sulfate, which can enter other markets rather than being discarded as waste. (11) The other precursor for this reaction, ferric chloride, can be synthesized in its hydrated form by recycling spent steel pickling liquor (contains hydrochloric acid) with scrap iron. However, it is necessary to dehydrate the hydrated ferric chloride to provide a suitable precursor for ferric fluoride production. The dehydration methods known are not practical. Dehydration by thermal treatment produces a low yield, while dehydration with a dehydrating agent such as thionyl chloride uses hazardous reactants and is costly. The issues associated with both dehydration processes prevent the use of ferric chloride produced by recycling steel pickling liquor. Instead, anhydrous ferric chloride is produced by oxidizing red hot iron with chlorine gas. (11) This process has a large yield and generates hydrogen chloride as a waste product. The produced anhydrous hydrogen fluoride (HF) is passed over anhydrous ferric chloride ($FeCl_3$) in a heated, oxygen-free reactor to produce FeF_3 . (2)

3. Synthesis of FeF_3 from Fe-only pickling liquor

Production of ferric fluoride from spent pickling liquor can be split into two steps: the synthesis of $\beta\text{-FeF}_3\cdot 3\text{H}_2\text{O}$ from SPL and the dehydration of $\beta\text{-FeF}_3\cdot 3\text{H}_2\text{O}$ to FeF_3 . Two practices employed in industry to prepare $\beta\text{-FeF}_3\cdot 3\text{H}_2\text{O}$ are evaporation or membrane filtration in conjunction with crystallization. During evaporation, the spent liquor is heated to its boiling point to remove excess acids and water while increasing the iron concentration to 80 - 120 kg/m^3 of SPL. (12) (13) This concentration is required to form a super saturated solution that will later be crystallized. Membrane filtration produces results similar to evaporation. First, microfiltration eliminates large solids from the solution and then, nanofiltration separates metal ions from the free acids. The portion retaining metal ions is recirculated through the system multiple times to increase the iron concentration. (3) The supersaturated solution is then held at approximately 50°C to allow for the nucleation and growth of $\beta\text{-FeF}_3\cdot 3\text{H}_2\text{O}$ crystals. Additional hydrofluoric acid can also be added to supplement crystal growth.

Unlike evaporation or membrane filtration, low temperature crystallization has not yet been employed by industry. Pickling liquor is slowly cooled to about -40°C to precipitate ice and $\text{FeF}_3\cdot 3\text{H}_2\text{O}$ crystals, which can then be separated by suction filtration. (4) These three possible routes to synthesize $\beta\text{-FeF}_3\cdot 3\text{H}_2\text{O}$ are highlighted in the upper portion of Figure 3. However, because the solutions in this paper are synthetically prepared to specific concentrations, these techniques are not studied in detail. They are only mentioned to describe the conversion process from pickling liquor to FeF_3 in its entirety.

The $\beta\text{-FeF}_3\cdot 3\text{H}_2\text{O}$ crystals are then converted to FeF_3 by thermal decomposition as highlighted in the lower portion of Figure 3. The specific temperatures for decomposition are discussed herein. In this study, sample pickling liquors containing iron as the only metallic species were prepared to establish a comparative baseline. The solution was initially composed of the composition Fe SPL A in Table 1, but this process resulted in a very low yield of fabrication. The composition was therefore altered to the composition Fe SPL B in Table 1 which improved yield to about 27% moles of precipitated $\beta\text{-FeF}_3\cdot 3\text{H}_2\text{O}$ after one week of reaction based on original concentration of Fe in the solution. The fabricated crystals were single phase and identified as $\beta\text{-FeF}_3\cdot 3\text{H}_2\text{O}$ by x-ray diffraction analysis as shown in Figure 4.

DSC analysis was performed to study the characteristics of decomposition during dehydration. Figure 5 reveals the transformation of $\beta\text{-FeF}_3\cdot 3\text{H}_2\text{O}$ to FeF_3 occurs in a single, large endothermic decomposition step at approximately 140.47 °C while the small bump at 97.32°C could be associated to the evaporation of adsorbed water. As a result, heat treatments were performed at various temperatures above 140°C under flowing Ar with the goal to dehydrate $\beta\text{-FeF}_3\cdot 3\text{H}_2\text{O}$ into FeF_3 . A first sample was heat-treated at 200°C for two hours, which resulted in the decomposition of $\beta\text{-FeF}_3\cdot 3\text{H}_2\text{O}$ into a hydrate of lower water content $\text{FeF}_3\cdot 0.33\text{H}_2\text{O}$ and small amounts of anhydrous FeF_3 (Fig. 6). A second sample was then heat-treated at higher temperature. At 400°C, dehydration was driven further and the sample consisted mostly of anhydrous FeF_3 with a very small amount of $\text{FeF}_3\cdot 0.33\text{H}_2\text{O}$ (Fig. 6). The residual $\text{FeF}_3\cdot 0.33\text{H}_2\text{O}$ phase could result from reaction of FeF_3 with ambient air upon transfer from the tube furnace to a He-filled glove box. Finally, a third sample was submitted to two successive 2-hour heat-treatments at 150°C and 400°C leading to successful dehydration with complete transformation into single phase FeF_3 (Fig. 7). Table 2 shows the lattice parameters of the FeF_3 materials synthesized from SPL B are consistent with JCPDS values and close to that obtained from a commercial source. In addition, the material we fabricated is of lower crystallinity than FeF_3 obtained from a commercial source with 38nm crystallite size compared to 62nm for the commercial sample.

After heat treatment at 400°C, the sample was observed to be of an orange-brown color rather than the characteristic light green color of commercial FeF₃. It is possible an oxide layer has formed on the surface of the powder. However, the lack of evidence for such oxide by XRD analysis most likely stems from amounts below detection limit. To further identify if this oxide layer exists at the surface, a sample was submitted to three consecutive heat-treatments at 150°C, 400°C and 450°C respectively. Figure 7 shows that heating from 400°C to 450°C results in the growth of Fe₂O₃. Additionally, the color of the sample changes to a slightly darker shade of orange-brown. Finally, because the position of the FeF₃ peaks do not shift after heat treatment, there is indication that surface oxidation is occurring rather than oxidation within the crystal lattice. Small amounts of surface oxidation are expected to be a benefit to the ultimate electrochemical processes.

4. Synthesis of FeF₃ and CrF₃ from Fe-Cr-Ni pickling liquor

In order to more accurately replicate pickling liquors obtained from the stainless steel fabrication process, chromium and nickel metal species were added to generate pickling liquors of composition Fe-Cr-Ni SPL from Table 1. The composition is derived from a metals ratio of 36:5:9 Fe:Ni:Cr and a metals concentration of 60g/L. (4) The solution is prepared and stored for one week to allow for crystallization to occur. After crystallization was complete, a yield of nearly 29% was obtained, assuming both FeF₃·3H₂O and CrF₃·3H₂O precipitate out of solution. This value is similar to that obtained with pure iron solutions.

X-ray diffraction analysis (Fig. 8) of the crystals obtained after crystallization reveals the presence of β-FeF₃·3H₂O and, CrF₃·3H₂O or α-FeF₃·3H₂O. Since CrF₃·3H₂O is isostructural to the α-FeF₃·3H₂O phase, distinction between both phases is difficult. (14) However, it should be noted that α-FeF₃·3H₂O is a disordered metastable phase whose crystal structure reorients into β-FeF₃·3H₂O over an extended period of time or at elevated temperatures and no alpha phase was identified in our previous precipitations without the presence of Cr. (15) Therefore, we believe it could be possible to distinguish between both phases after heat treatment.

DSC analysis, shown in Figure 9, reveals that the decomposition of the mixture of β-FeF₃·3H₂O with CrF₃·3H₂O or α-FeF₃·3H₂O into FeF₃ occurs in two closely spaced endothermic decomposition steps at approximately 146.96 °C and 166.45°C respectively. The first step correlates to the decomposition of β-FeF₃·3H₂O while the second step could correlate to the decomposition of CrF₃·3H₂O or α-FeF₃·3H₂O. A small bump before the main peak at 96.88°C can be associated to the evaporation of adsorbed water.

As performed with the pure β-FeF₃·3H₂O samples reported above, samples were heated above the decomposition temperatures obtained by DSC. As with the optimized pure Fe fluoride hydrates, the samples were heat-treated at 150°C for 2 hours to allow for the initial dehydration step, then at 400°C for 5 hours to form the final product. The resulting XRD scan reported in Figure 10 reveals single phase FeF₃. Lattice parameters (Table 2) are similar to that obtained with the Fe-only pickling solution and consistent with JCPDS values for rhombohedral FeF₃. The synthesized material shows wider diffraction peaks than the ones obtained with the commercial FeF₃ consistent to a lower crystal size of 41nm obtained by Rietveld refinement.

Since x-ray diffraction does not present any evidence for any distinct Cr-based phase, we can hypothesize on the possibility of the formation of a chromium- iron solid solution during crystallization. The later would be consistent with the Hume-Rothery rules determined from the similarity in atomic radii and

electronegativity of chromium (0.62\AA) and iron (0.65\AA) ions in the 3+ state. (16) This would also be consistent with a previous report of $\text{Cr}_{0.5}\text{Fe}_{0.5}\text{F}_3$ solid solutions fluorides. (17) As shown in Table 3, quantitative EDS analysis of the sample synthesized from Fe-Cr-Ni pickling liquor confirmed the material comprises iron, chromium, fluorine, and oxygen however no nickel was detected. The Fe:Cr elemental ratio is calculated from the relative atomic percents of Fe and Cr resulting in a value of approximately 3.747:1. This is incorporated into chemical formula of ferric fluoride to give a composition of $\text{Fe}_{0.79}\text{Cr}_{0.21}\text{F}_3$. Field emission electron microscopy (FESEM) analysis of the final product revealed a wide distribution of crystal shape and sizes (Fig. 11). Furthermore, even though X-ray analysis does not indicate the presence of any oxide phase, through visual identification of the color change it can be concluded that an oxide coating has formed on the surface of the iron-chromium fluoride particles as similarly mentioned above for the pure FeF_3 sample.

5. *Electrochemical Performance*

As demonstrated above, anhydrous iron fluoride has been successfully synthesized from iron based pickling liquors through successive heat-treatments under argon. The samples tested for electrochemical activity were synthesized through a succession of two heat-treatment at 150°C for two hours and at 400°C for five hours. Both the materials obtained from Fe-only and Fe-Ni-Cr liquors were evaluated and compared to commercial FeF_3 after formation into nanocomposites. Figure 12 presents the second cycle voltage profiles obtained at 60°C with a current of 7.5mA/g based on the weight of the nanocomposite. Both materials fabricated from pickling liquors are electrochemically active and exhibit discharge profiles similar to that of commercial FeF_3 , except for the slightly lower capacity of the Fe-Cr-Ni sample. All capacities obtained exceeded 75% of theoretical values inclusive of the $\text{FeF}_3 \rightarrow \text{Li}_{0.5}\text{FeF}_3 \rightarrow \text{LiFeF}_3$ insertion reaction above 3V and the $\text{LiFeF}_3 \rightarrow 3\text{LiF} + \text{Fe}$ conversion reactions at approximately 2V. No distinct electrochemical signatures originating from CrF_3 or NiF_2 could be abstracted from the voltage profile.

Discharge capacity per gram of FeF_3 was plotted as a function of cycle number in Figure 13. Both samples fabricated from pickling solution showed improved capacity retention compared to the commercial material. Best results were obtained with the sample derived from the Fe-Cr-Ni solution. In addition, rate capability was tested with the material synthesized from the iron only pickling liquor.

6. *Environmental calculations*

6.1. *Disposal of Spent Pickling Liquor*

The process of spent pickling liquor disposal was summarized in in Figure 1 while Table 4 presents the quantities of input as well as the output materials involved in the disposal process. The values in Table 4 are calculated supposing stoichiometric reactions. However, an excess of the hydroxide ion is included in this table to ensure mass balance even though it forms water by neutralizing the acids. Using these assumptions, the estimated environmental impact for SPL disposal is 745 PEI/L of SPL. Since values for this section are given in units of PEI/L of SPL and the theme of units used throughout this paper is PEI/kg of FeF_3 , the above value can be converted into ~ 23281 PEI/kg of FeF_3 . This is accomplished with a conversation factor that 1 L of SPL has the potential to yield 0.032 kg of FeF_3 (or $(\text{Fe,Cr})\text{F}_3$). The derivation of this factor is explained in detail in Section 6.3 below. Major contributing elements to this calculation are associated to the calcium and nitrate ions remaining in the wastewater, which mainly have

aquatic toxicity effects. The energy contribution is assumed to be minimal because the neutralization process does not require relatively demanding mixing or filtering technology.

6.2. Production of Anhydrous Ferric Fluoride via current commercial synthesis process

The commercial production of anhydrous FeF_3 was presented in Figure 2 while Table 5 shows the material flow used to estimate the environmental impact of production of ferric fluoride. The estimated environmental impact for ferric fluoride production is 1.273 PEI/kg of FeF_3 . The chemical component, which has a value of 1.2662 PEI/kg of FeF_3 , greatly outweighs the energy component, which has a value of 0.0068 PEI/kg. This occurs because of the high toxicity of the outputs, specifically hydrogen chloride gas which is released into the environment. Specific assumptions for this PEI calculation are that fluor spar is primarily calcium fluoride and the synthesis of ferric fluoride from its precursors is stoichiometric with a two percent loss of ferric chloride. (18)

6.3. Production of $(\text{Fe,Cr})\text{F}_3$ from Spent Pickling Liquor

As described above, production of $(\text{Fe,Cr})\text{F}_3$ from spent pickling liquor can be split into two steps: crystallization of the hydrate from SPL and dehydration to $(\text{Fe,Cr})\text{F}_3$. The composition of SPL used in this paper allows for crystallization to favorably occur without any added chemicals or energy. The various techniques of crystallization mentioned above incorporate an amount of energy with an environmental cost comparatively negligible to the rest of the system. Therefore, the only contributing factor to environmental cost from the crystallization step is disposal of the effluent remaining after crystallization. The exact composition of this liquid is unknown. However, by calculating backwards from the estimated crystal yield and crystal composition, the remaining liquid composition is estimated to be 30.7g/L $[\text{Fe}^{3+}]$, 7.7g/L $[\text{Cr}^{3+}]$, 6g/L $[\text{Ni}^{2+}]$, 43.6g/L $[\text{F}^-]$, and 195g/L $[\text{NO}_3^-]$. Slight fluctuations in this calculation should not have a major effect on PEI. The worst case scenario for disposing this effluent is through lime neutralization. Table 6 below shows the stoichiometrically calculated material flow used to estimate the PEI. The estimated environmental impact for this method of crystallization effluent disposal is 727.7 PEI/L of SPL.

The dehydration step of the $(\text{Fe,Cr})\text{F}_3$ crystalhydrate follows a simple thermal decomposition process. Argon gas is introduced into a furnace to remove ambient air and the furnace is incrementally heated to 400°C for extended periods of time. The main source of environmental impact for this step is the energy required to heat the furnace. The environmental impact of the process gas is assumed to be negligible because it is often a byproduct of other gas refining processes. The impact of heating is estimated from the required enthalpy for transformation given by the DSC shown in Figure 9. The enthalpy is approximately 16.313 kJ/gram of crystalhydrate. Thus, the potential environmental impact for dehydration is 0.16 PEI/kg of $(\text{Fe,Cr})\text{F}_3$.

Before the combined PEI for the entire conversion process can be calculated, the units / L of SPL need to be adjusted into is / kg of $(\text{Fe,Cr})\text{F}_3$. This is accomplished by calculating the amount of metal fluoride hydrates present in the proposed solution and then adjusting the value according to the yield obtained through experimental trials. Finally, the hydrated form of the crystal must be converted to its dehydrated form. Therefore, 1 L of SPL has the potential to yield 0.032 kg of $(\text{Fe,Cr})\text{F}_3$. The new PEI for the

crystallization step is ~ 22740 PEI/kg of $(\text{Fe,Cr})\text{F}_3$. The combined PEI for the whole conversion process is roughly the same value because thermal decomposition does not contribute much to environmental impact.

Discussion

Crystallization from iron only pickling solutions proved that an appreciable yield of nanocrystalline $\beta\text{-FeF}_3 \cdot 3\text{H}_2\text{O}$ could relatively rapidly be produced. The crystallization process efficiency could be further improved by optimization of temperature control, crystallization time, crystal seed introduction, and HF concentration. Forsberg and Rasmuson demonstrated that the crystal growth of iron fluoride trihydrate can be optimized at a temperature of 50°C , which in turn results in a higher yield. (19) Additionally, basic crystal growth kinetics indicate that if the sample pickling liquor was allowed to crystallize for a longer time period, then a larger yield of $\beta\text{-FeF}_3 \cdot 3\text{H}_2\text{O}$ is produced because there is more time to reach thermodynamic equilibrium. Furthermore, the same result can be achieved by the addition of seed crystals which provide sites of reduced surface energy for growth. Finally, we performed preliminary experiments indicating adding additional concentrated HF to sample pickling liquor would result in not only a dramatically increased yield, but also a shorter crystallization time. The tradeoff to this approach is that precipitate composition could change dependent on the altered solubility of the metal ions in solution.

Thermal treatment at 400°C was demonstrated to be effective in converting $\beta\text{-FeF}_3 \cdot 3\text{H}_2\text{O}$ into FeF_3 , but with a potential slight oxidation of the surface. The synthesized FeF_3 material successfully demonstrated electrochemical activity similar to that of a commercial source and approached theoretical values. In addition, the material obtained from pickling liquor also provided improved capacity retention upon cycling compared to the commercial sample. Such results may stem from the presence of an oxide surface layer based on previous results that demonstrated the benefits of the introduction of oxygen into the iron fluoride. (20)

Using a similar method, nanoparticles of FeF_3 with a small fraction of CrF_3 in solid solution were fabricated from Fe,Cr,Ni-pickling liquors. Such material was observed to also be electrochemically active, although of slightly lower capacity than FeF_3 , but of further improved capacity retention. Further optimization of this cathode material is possible through refinement of the techniques of Badway et al. and Yabuuchi et al. which could result in a higher capacity battery material with improved cycling capabilities. (21) (22)

The ability to form solid solutions with various contents of Cr provides tuneability that is important to describing the potential environmental impact of the conversion process as the composition of the waste generated is directly related to the composition of the material crystallized. If SPL is composed mostly of a high concentration of chromium, then the potential environmental impact for disposal or conversation would be much higher because of chromium's much enhanced toxicity compared to Fe. However, for the sake of this paper, the composition of the waste generated by converting SPL into $(\text{Fe,Cr})\text{F}_3$ through crystallization is assumed to be 30.7g/L $[\text{Fe}^{3+}]$, 7.7g/L $[\text{Cr}^{3+}]$, 6g/L $[\text{Ni}^{2+}]$, 43.6g/L $[\text{F}^-]$, and 195g/L $[\text{NO}_3^-]$. From this information the estimated environmental impact for converting SPL into $(\text{Fe,Cr})\text{F}_3$ can be calculated. It should be noted that this calculation is solely composed of the disposal of the effluent produced from a conversion process which yields 29% of $(\text{Fe,Cr})\text{F}_3$. Any additional processing steps are ignored because of the very little amount of energy or added chemicals required to complete them.

The worst case scenario for disposal of the conversion effluent is through lime neutralization. Table 7 compares the potential environmental impact of this process with the current practices of SPL disposal and new FeF_3 production. The current practices produce battery material with a slightly increased environmental cost, indicating that the worst case scenario for converting SPL into iron fluorides is only marginally more environmentally sound. However, this margin can be dramatically increased through optimization of the conversion process as all our calculated values were based on an assumption of <30% yield. Simple adaption of the crystallization techniques mentioned above of iron-only pickling solutions to fit Fe,Cr,Ni-pickling liquors will have a significant impact on the yield. Table 8 shows the relationship that increased crystallization yield has on reduction of the environmental impact. This table is created by following the procedure highlighted in Section 6.3 above and assumes additional environmental costs associated with achieving the higher crystallization yield are insignificant. It shows that the increased efficiency means that more $(\text{Fe,Cr})\text{F}_3$ is produced, less pickling liquor is discarded as waste, and a lower PEI is generated, indicating a very significant lower environmental impact. This clearly demonstrates the significant impact of yield on the environmental and likely economic costs and should be a focus of future research. The optimization further highlights how SPL conversion is the more environmentally-friendly technology. The next paragraph highlights a possible best case scenario to forecast the uppermost potential of this technology.

A best case scenario would be to effectively create a closed loop process to recycle the conversion effluent and minimize environmental impact. One approach proposed by a group at Complutense University of Madrid recommends the use of KF and KOH as a reagent to selectively precipitate iron and chromium in fluoride salts. Followed by hydrolysis of the precipitates and neutralization of the effluent, this process produces $\text{Fe}(\text{OH})_3$, $\text{Cr}(\text{OH})_3$, and $\text{Ni}(\text{OH})_2$ as solids and a solution of K^+ , F^- , and NO_3^- ions that can later be treated by membrane filtration to recover valuable acids. (23) The focus of their process is to recycle acids back towards pickling and recover nickel as a marketable good. A slight modification of their process through the use of HF as a reagent would shift focus towards the production of $\text{FeF}_3 \cdot 3\text{H}_2\text{O}$ and $\text{CrF}_3 \cdot 3\text{H}_2\text{O}$, precursors necessary for battery material production. Subsequent dehydration of the crystal hydrates would produce desired cathode material. This process would remove much of the metal ions in solution and produces a waste composed of hydrofluoric and nitric acid that needs to be reconstituted with new acids before being returned into fresh pickling liquor stream. The only contributing factors to the environmental impact would be the production of the acids and energy, which have a negligible impact when compared to what is saved from the lack of SPL disposal.

While we demonstrated that spent pickling liquor similar to that obtained by stainless steel manufacturers can be transformed into a metal fluoride material that can be used as a cathode material for lithium batteries and that such process is more environmentally friendly than current practices for the disposal of the spent liquor and iron fluoride fabrication, we are well aware that costs as well as demand will drive the adoption of the proposed process. As a result we decided to briefly touch on the subject of costs without going into detail, as it would fall out of the scope of this manuscript. From the stainless steel industry perspective, even if the spent pickling liquor were donated tremendous savings would be associated to the elimination of the disposal process. From the battery manufacturer, savings would be associated to lower costs for an iron fluoride material of potentially improved electrochemical performance. Lower iron fluoride fabrication costs would derive from the elimination of the anhydrous HF-based process that requires capital-intensive installations due to the corrosive HF gas, as well as high utility and maintenance costs. Overall, the proposed process would not only be more environmentally

sound but it would also bring about tremendous savings to both industries. The battery manufacturers' economical benefits would also increase as the conversion process is optimized. Finally, ultimate cost savings would be optimized by collocating the facilities for the conversion of the SPL near stainless steel plants where spent liquor is produced in order to reduce transport costs, both economic and environmental.

Conclusion

It has been demonstrated that it is possible to convert spent pickling liquor into a viable battery material through environmentally beneficial process of crystallization and dehydration. Anhydrous FeF_3 of similar electrochemical performance to a commercially derived FeF_3 has been established using compositions similar to the effluent of the stainless steel pickling process. Even though this material shows improved capacity retention compared to commercial FeF_3 , much can be done to further the performance of the material such as forming nanocomposites with a conductive matrix in-situ during the crystallization process, incorporation of oxygen and optimization of transition metal substitution, as demonstrated in the literature. The use of the stainless steel effluent as a source raw material for the fabrication of iron based transition metal fluorides may be of great benefits to both industries and the environment in the future as the process represents a decrease in overall environmental impact, and economic cost as a waste product is transformed into a value added product. For the stainless steel industry, savings would come in the form of dramatically lower disposal costs, while the battery manufacturers' economical benefits would stem from lower material cost.

Acknowledgements

The authors would like to acknowledge the Rutgers Energy Institute and the Rutgers University Energy Storage Research Group for financial support.

References

1. N. Pereira, F. Badway, M. Wartelsky, S. Gunn, G. G. Amatucci, *J. Electrochem. Soc.*, 2009, **156**, A407-A416 .
2. *US Pat.*, US4938945, 1988
3. K. Tjus, R. Bergstrom, U. Fortkamp, K. Forsberg, A. Rasmuson, *Development of a Recovery System for Metals and Acids from Pickling Baths using Nanofiltration and Crystallization*, IVL Swedish Environmental Research Institute Ltd., Stockholm, 2006.
4. M. Sartor, D. Buchloh, F. Rogener, T. Reichardt, *Chem. Eng. J.*, 2009, **153**, 50-55.
5. S. Myung, S. Sakurada, H. Yashiro, Y. Sun, *J. Power Sources* , 2013, **223**, 1-8.
6. L. Liu, H. Guo, M. Zhou, Q. Wei, Z. Yang, H. Shu, X. Yang, J. Tan, Z. Yan, X. Wang, *J. Power Sources*, 2013, **238**, 501-515.
7. F. Badway, N. Pereira, F. Cosandey, G.G. Amatucci , *J. Electrochem. Soc.*, 2003, **150**, A1209-A1218.
8. *US Pat.*, US5418091, 1995
9. *US Pat.*, US4938945, 1988
10. P. Patnaik, *Handbook of Inorganic Chemicals*, McGraw-Hill, New York, 2003.
11. *Large Volume Inorganic Chemicals- Ammonia, Acids and Fertilizers*, European Commission Institute for Prospective Technological Studies Sustainability in Industry, 2007.
12. *US Pat.*, US4252602, 1981
13. J. B. Stephenson, J. C. Hogan and R. S. Kaplan, *Environ. Prog.*, 1984, **3**, 50-53.
14. F. H. Herbstein, M. Kapon, G. M. Reisner, *Zeitschrift für Kristallographie*, 1958, **171**, 209-224.
15. D. G. Karraker, P. K. Smith, *Inorg. Chem.*, 1991, **31**, 1118-1120.
16. B. Adamczyk, A. Hess, E. Kemnitz, *J. Mater. Chem.*, 1996, **6**, 1731-1735
17. I. Plitz, F. Badway, J. Al-Sharab, A. DuPasquier, F. Cosandey, G. G. Amatucci, *J. Electrochem. Soc.*, 2005, **152**, A307-A315 .
18. Commercial Source
19. K. Forsberg, A. Rasmuson , *J. Cryst. Growth*, 2006, **296**, 213-220.
20. W. Zhang, L. Ma, H. Yue Y. Yang, *J. Mat. Chem.*, 2012, **22**, 24769-24775.
21. F. Badway, N. Pereira, F. Cosandey, G.G. Amatucci , *J. Electrochem. Soc.*, 2003, **150**, A1318-A1327.
22. N. Yabuuchi, M. Sugano, Y. Yamakawa, I. Nakai, K. Sakamoto, H. Muramatsu, S. Komaba, *J. Mat. Chem.*, 2011, **21**, 10035-10041.
23. J. Hermoso, J. Dufor, J. L. Galvez, C. Negro, F. Lopez-Mateos, , *Ind. Eng. Chem. Res.*, 2005, **44**, 5750-5756.
24. Stainless Steel Manufacturer
25. *Additional Information submitted during information exchange on Large Volume Inorganic Chemicals- Solids and Other Industry*, European Commission Institute for Prospective Technological Studies Sustainability in Industry, 2005.

Compositions of Spent Pickling Liquor					
Pickling Liquor	[Fe ³⁺] (g/L)	[Cr ³⁺] (g/L)	[Ni ²⁺] (g/L)	[NO ₃ ⁻] (g/L)	[F ⁻] (g/L)
Industrial SPL (23)	30-45	5-10	3-5	150-180	60-80
Fe SPL A	43.2	-	-	143.9	44.1
Fe SPL B (24)	78.9	-	-	258.7	80.7
Fe-Cr-Ni SPL (4)	42.2	10.8	6	195	60

Table 1- This table highlights the various compositions of spent pickling liquor discussed in this paper.

Source	Crystal Structure	a	C
JCPDS 01-088-2023	Rhombohedral	5.1941(9)	13.334(9)
Commercial FeF ₃	Rhombohedral	5.206(3)	13.287(3)
FeF ₃ from Fe SPL B	Rhombohedral	5.208(0)	13.352(8)
FeF ₃ from Fe-Cr-Ni SPL	Rhombohedral	5.201(2)	13.314(2)

Table 2- This table describes lattice parameters for samples discussed in paper, which are fit with Reitveld Refinement by the software TOPAS.

Element	Atomic Percent
C	4.12
O	7.85
F	58.74
Cr	6.17
Fe	23.12

Table 3- Atomic percent information obtained from EDS of the final (Fe,Cr)F₃ product

Inputs		Outputs					
SPL (L)	Ca(OH) ₂ (g)	Fe(OH) ₃ (g)	Cr(OH) ₃ (g)	Ni(OH) ₂ (g)	CaF ₂ (g)	Ca(NO ₃) ₂ (g)	OH ⁻ (g)
1	233.43	82.66	21.4	9.48	123.2	258.04	53.64

Table 4- Inputs and Outputs for SPL disposal used in the PEI Calculation

Inputs	Amount (kg/t FeF ₃)	Outputs	Amount (kg/t FeF ₃)
Fluorspar	1117.2-1170.4	CaSO ₄ (marketable coproduct)	1969.8
H ₂ SO ₄	1383.2-1436.4	CaSO ₄ (nonmarketable coproduct)	2.662-26.62
Fe (Scrap)	504.6	CaF ₂	3.19-37.24
Cl ₂	962.4	SO ₄ ²⁻	0.372-10.64
		Fluoride	0.0372-0.532
		Si	0.0532-0.532
		CO ₂	2.934-17.604
		H ₂	1.071-19.071
		Fe	0.07335-.7.335
		Zn	0.007335-2.2005
		Heavy Metals	<0.0007335-0.8802
		Solid Waste	7.335-51.345
		HCl	969.0
Total Energy	6.17-10.60 GJ/t FeF ₃	FeF ₃ , anhydrous	1000

Table 5-Inputs and Outputs for Ferric Fluoride Production used in the PEI Calculation (11) (25) (18)

Inputs		Outputs					
SPL (L)	Ca(OH) ₂ (g)	Fe(OH) ₃ (g)	Cr(OH) ₃ (g)	Ni(OH) ₂ (g)	CaF ₂ (g)	Ca(NO ₃) ₂ (g)	OH ⁻ (g)
1	201.48	58.75	15.25	9.48	89.53	258.04	53.43

Table 6 -Inputs and Outputs for crystallization effluent disposal used in the PEI Calculation

Scenario	Process	Potential Environmental Impact PEI/kg of Battery Material
Current Industry Practices	SPL Disposal	23281
	New FeF ₃ Production	1.27
	Total	23282.27
Worst Case Scenario	Conversion of SPL into (Fe,Cr)F ₃	22740

Table 7- Comparison of the potential environmental impact of each of scenario assuming a yield of 29% for the conversion of (Fe,Cr)F₃·3H₂O to (Fe,Cr)F₃

Crystallization Yield (%)	kg of (Fe,Cr)F₃/ L of SPL	Total PEI
29%	0.032	22740
40%	0.044	16400
50%	0.055	13010
60%	0.066	10750
70%	0.077	9140
80%	0.088	7940
90%	0.099	6990

Table 8- Effect of increasing crystallization yield on quantity of material and environmental impact

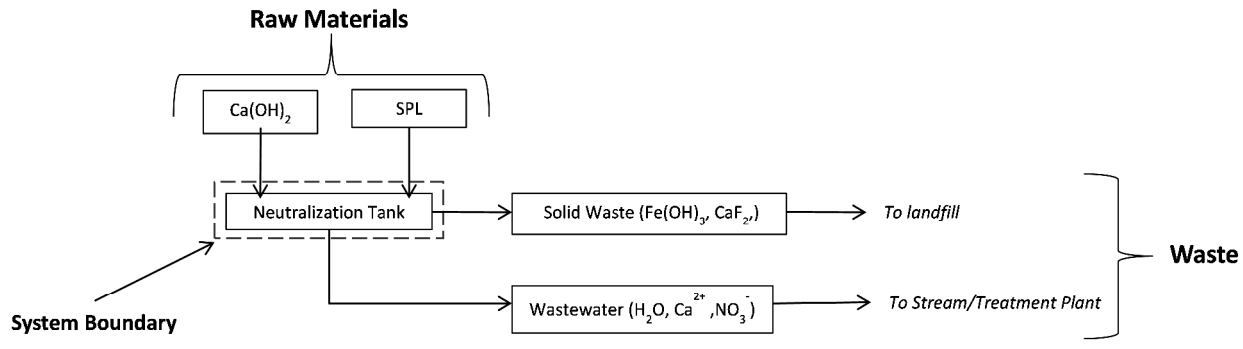


Figure 1- Material Flow Chart for Spent Pickling Liquor Neutralization

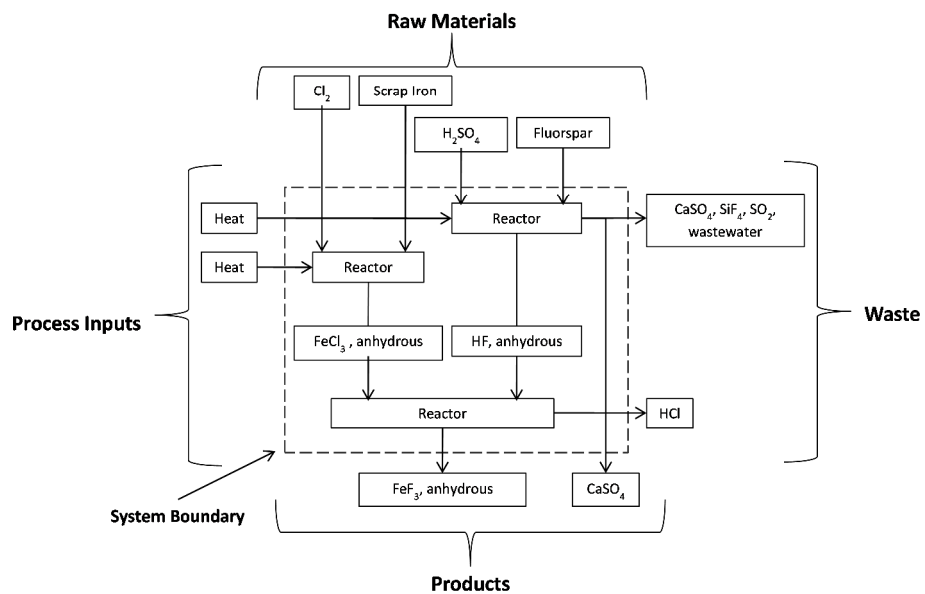


Figure 2- Material Flow Chart of Ferric Fluoride Production

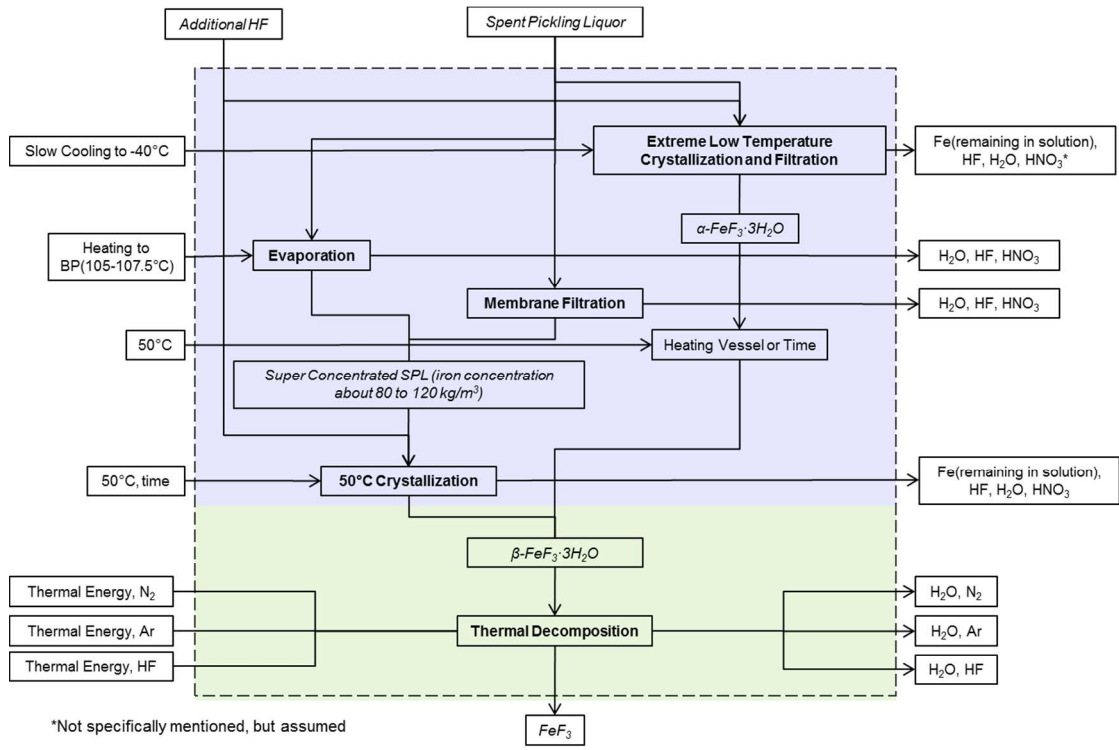


Figure 3- Material Flow Chart of Ferric Fluoride Production from Spent Pickling Liquor

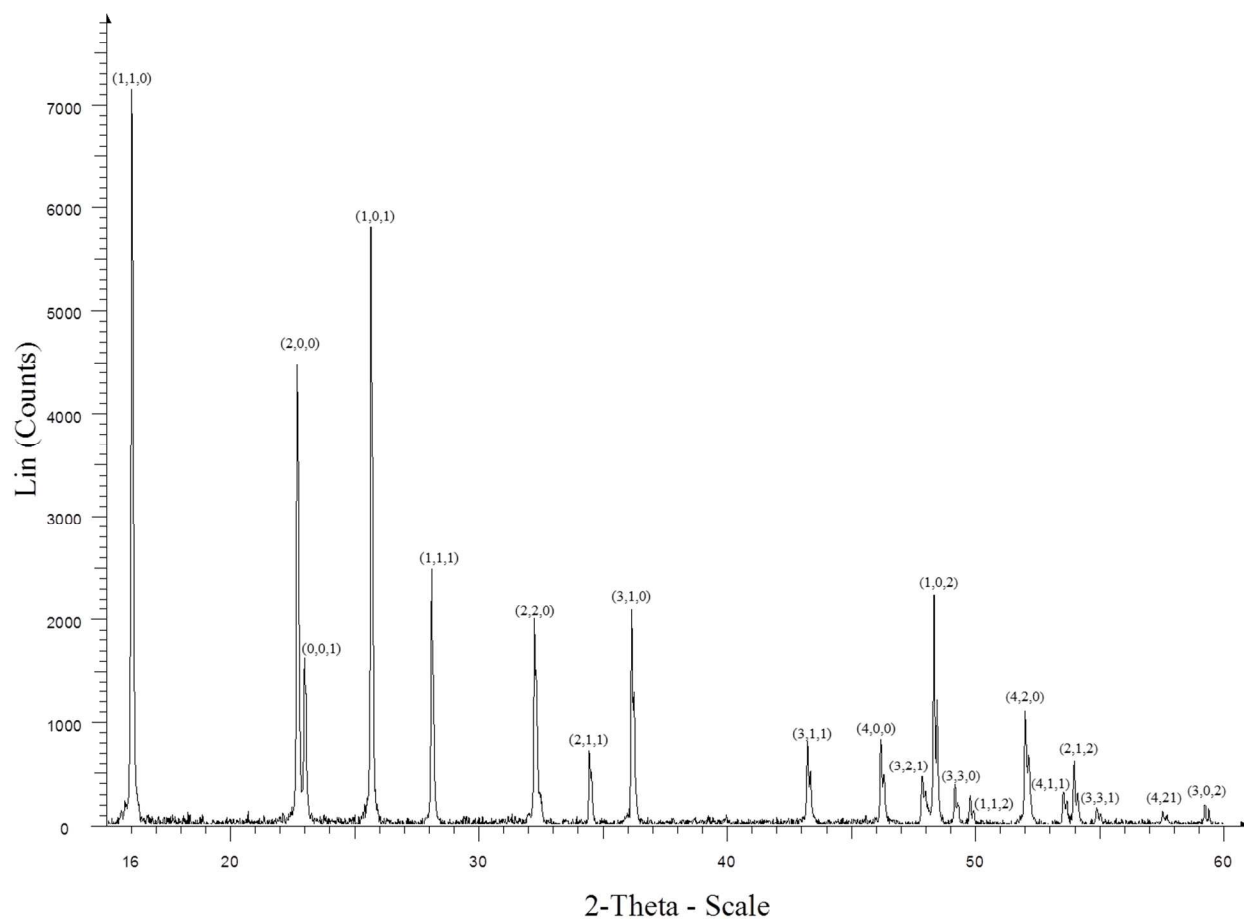


Figure 4 - XRD pattern of crystals precipitated from iron only pickling solution at room temperature. Peaks indexed are associated to β - $\text{FeF}_3 \cdot 3\text{H}_2\text{O}$ (JCPDS 00-032-0464)

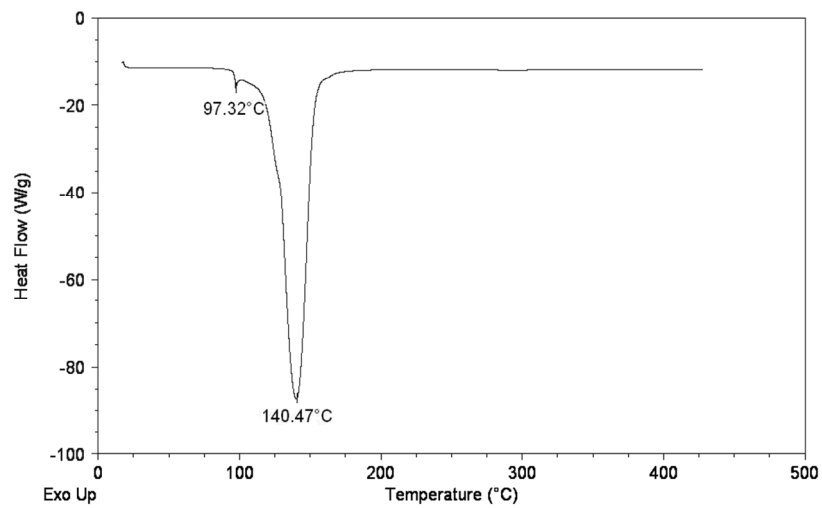


Figure 5 - DSC scan of $\beta\text{-FeF}_3\cdot 3\text{H}_2\text{O}$ to FeF_3 heated in helium from RT to 450°C at a rate of 5°C/min

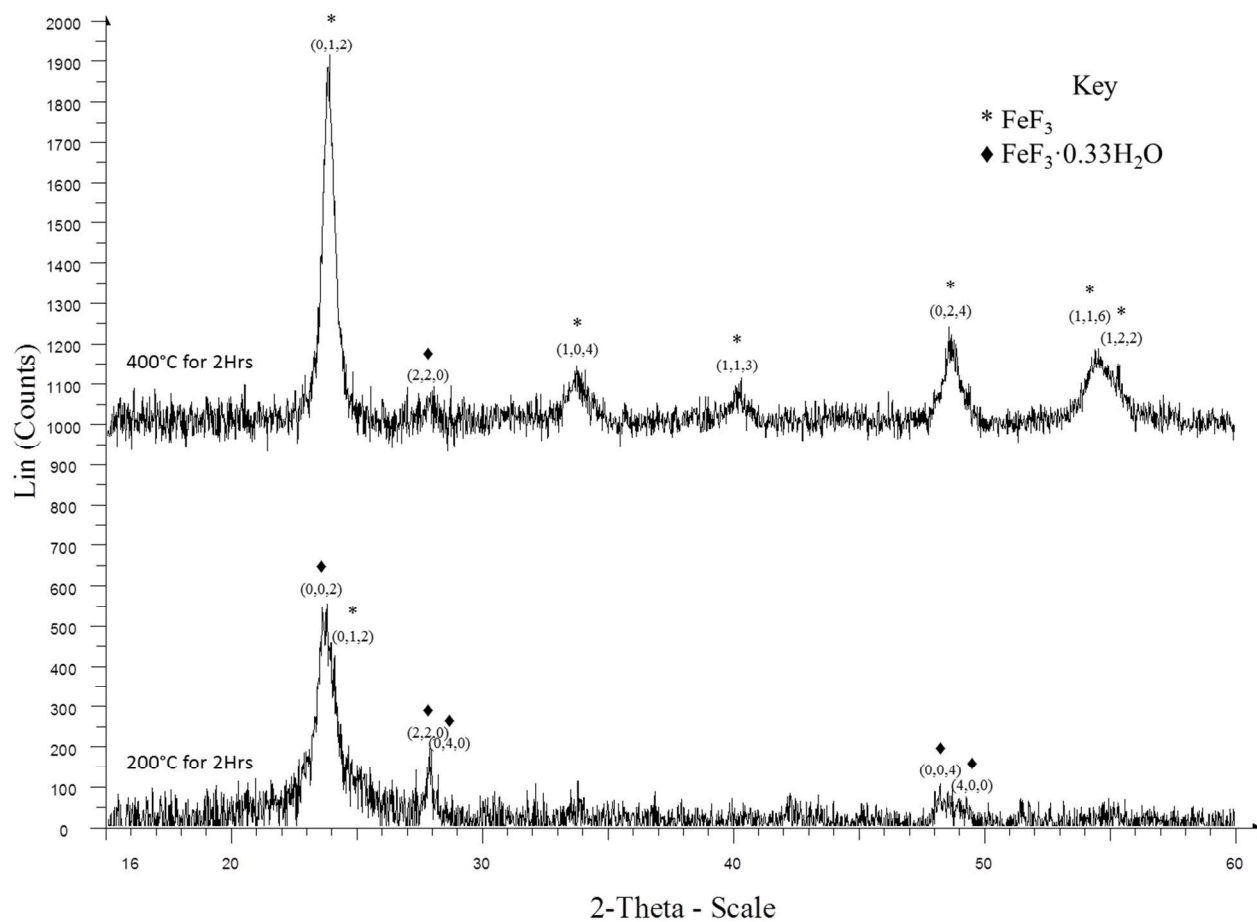


Figure 6- XRD pattern of the initial $\beta\text{-FeF}_3 \cdot 3\text{H}_2\text{O}$ sample after 2-hour heat-treatment at 200°C (bottom), and at 400°C (top). Peaks indexed by stars are consistent with FeF_3 (JCPDF 01-088-2023) and peaks indexed by diamonds are consistent with $\text{FeF}_3 \cdot 0.33\text{H}_2\text{O}$ (JCPDS 01-076-1262).

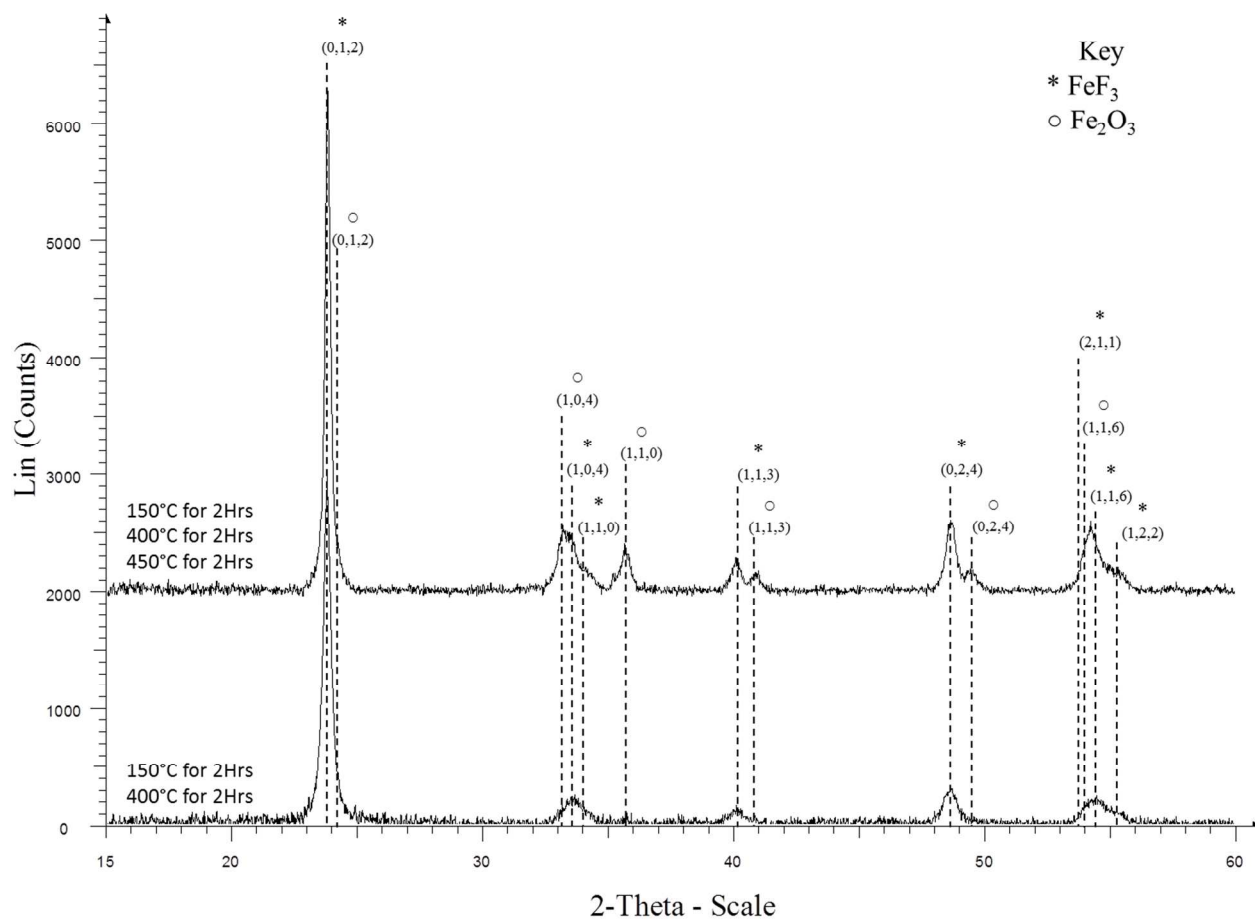


Figure 7- XRD scan of the $\beta\text{-FeF}_3\cdot 3\text{H}_2\text{O}$ sample submitted to two consecutive heat-treatments at 150°C and 400°C (bottom), and followed by a third heat-treatment at 450°C for two hours (top). Peaks indexed by stars are of FeF_3 (JCPDS 01-071-3710) and peaks indexed by empty circles are of Fe_2O_3 (JCPDS 00-089-0599).

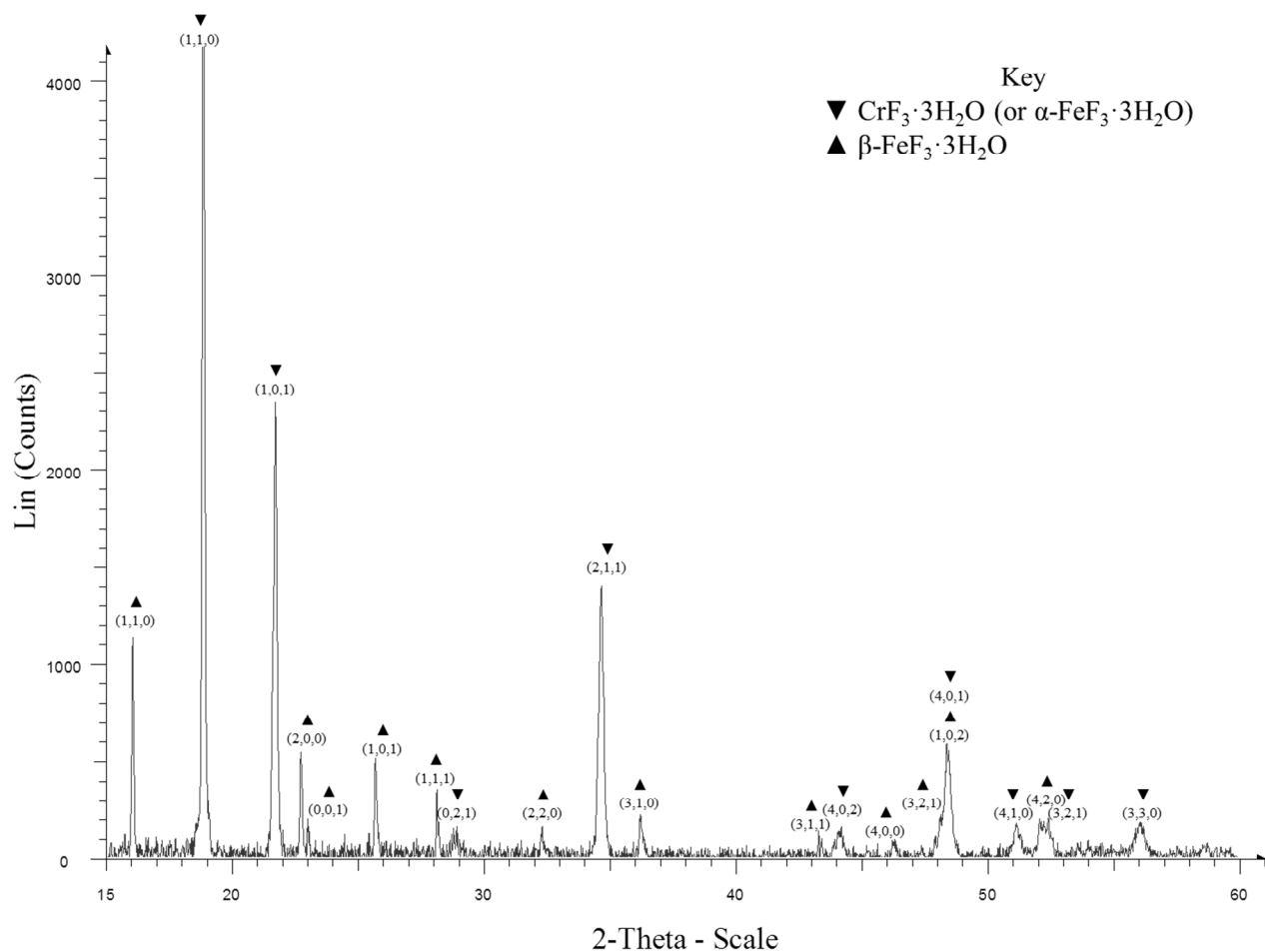


Figure 8- XRD pattern of crystals produced from the Fe, Ni, and Cr sample pickling liquors. Peaks marked by point-up triangles are of $\beta\text{-FeF}_3 \cdot 3\text{H}_2\text{O}$ (JCPDS 00-032-0464) and peaks marked by point-down triangles are of $\text{CrF}_3 \cdot 3\text{H}_2\text{O}$ (JCPDS 00-017-0316) or $\alpha\text{-FeF}_3 \cdot 3\text{H}_2\text{O}$ (JCPDS 00-024-0071).

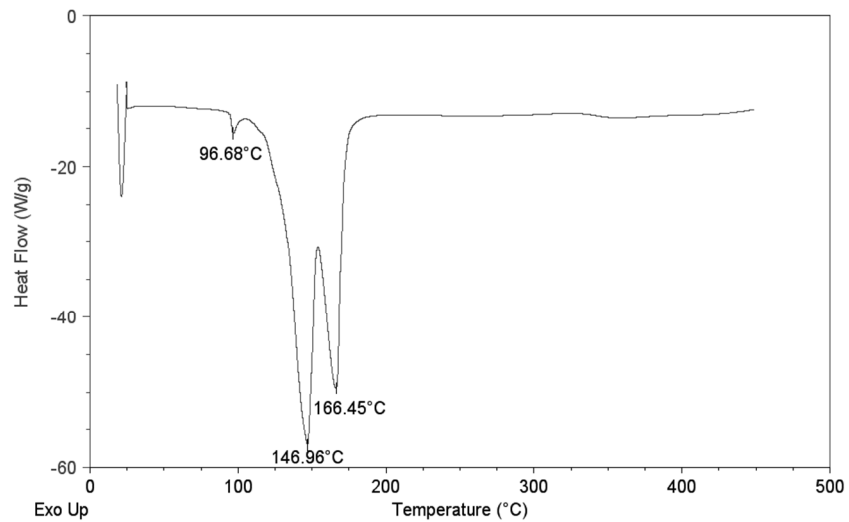


Figure 9- DSC scan of hydrated crystal sample from Fe-Cr-Ni SPL heated from RT to 450°C at a rate of 5°C/min

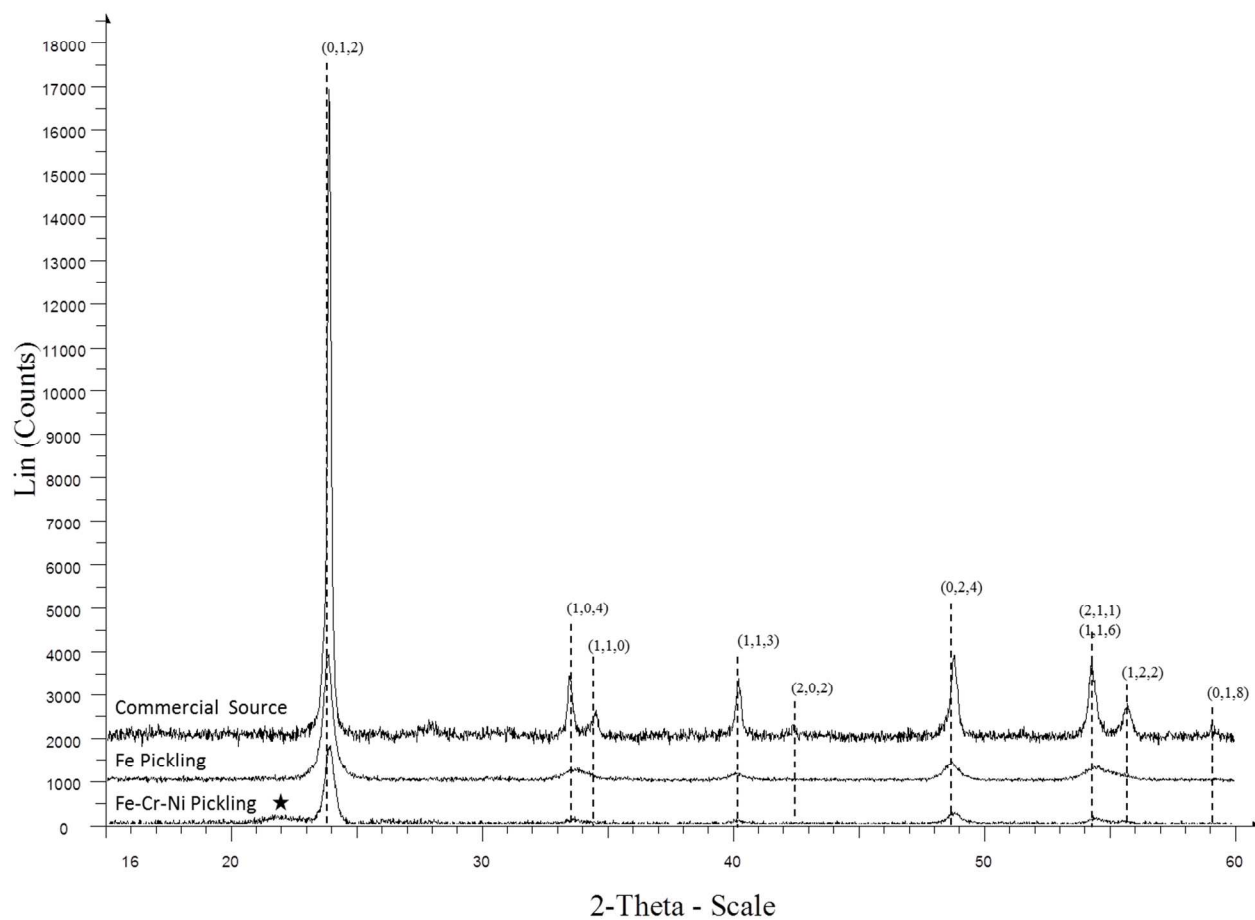


Figure 10- XRD patterns of crystals produced from the Fe- and the Fe-Cr-Ni pickling liquors heated at 150°C for two hours and then at 400°C for five hours, compared to a commercial FeF₃ material. Peaks indexed indicate FeF₃ (JCPDS 01-071-3710) while system peak is present in the Fe-Cr-Ni sample as shown by the star.

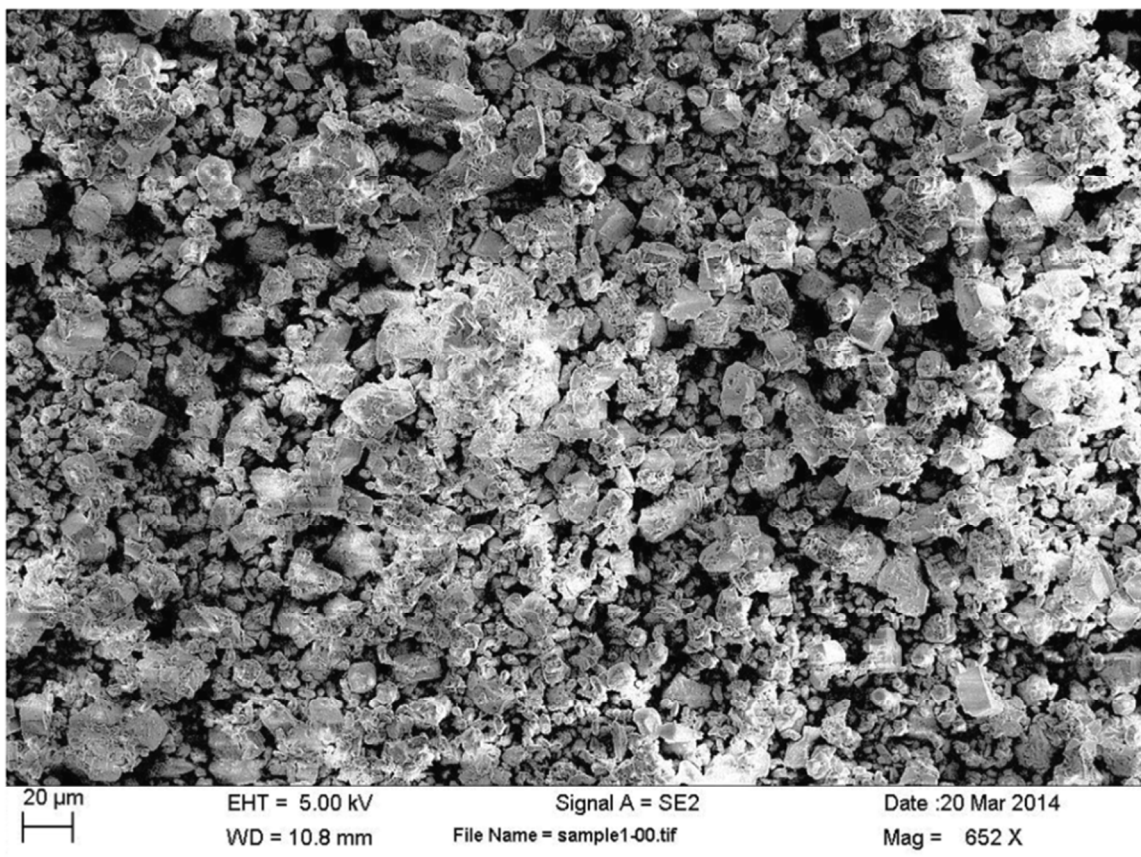


Figure 11- SEM image of the final (Fe,Cr)F₃ product at a x652 magnification.

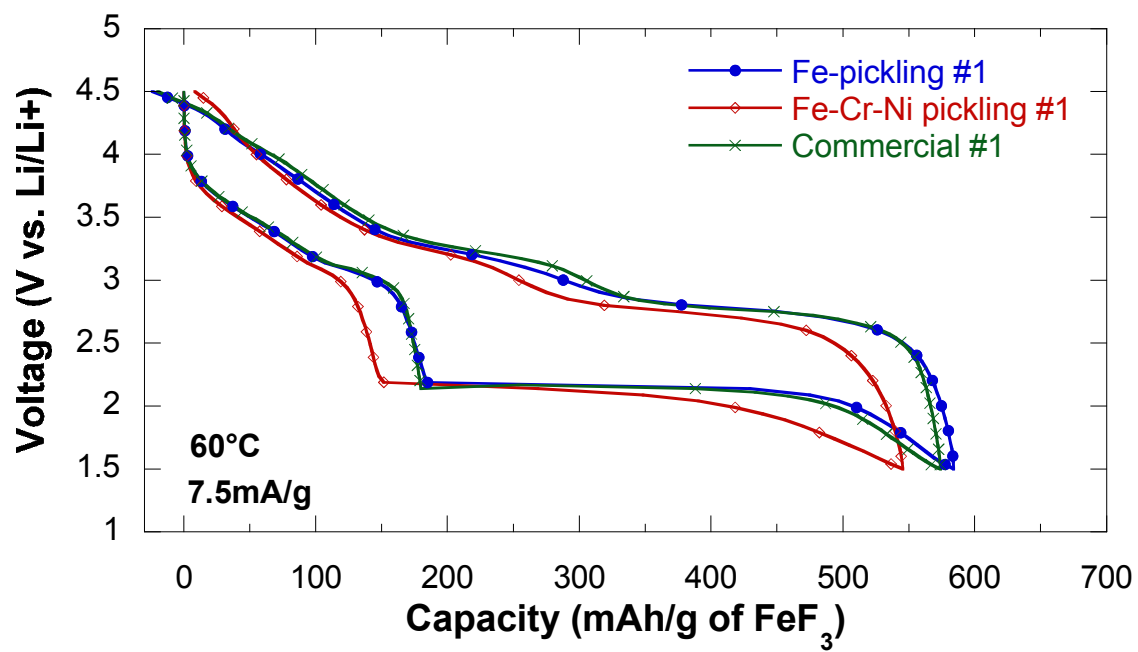


Figure 12- Second cycle voltage profile of the samples synthesized from pickling liquors compared to commercial FeF_3 performed at 60°C and 7.5 mA/g based on the weight of the nanocomposite

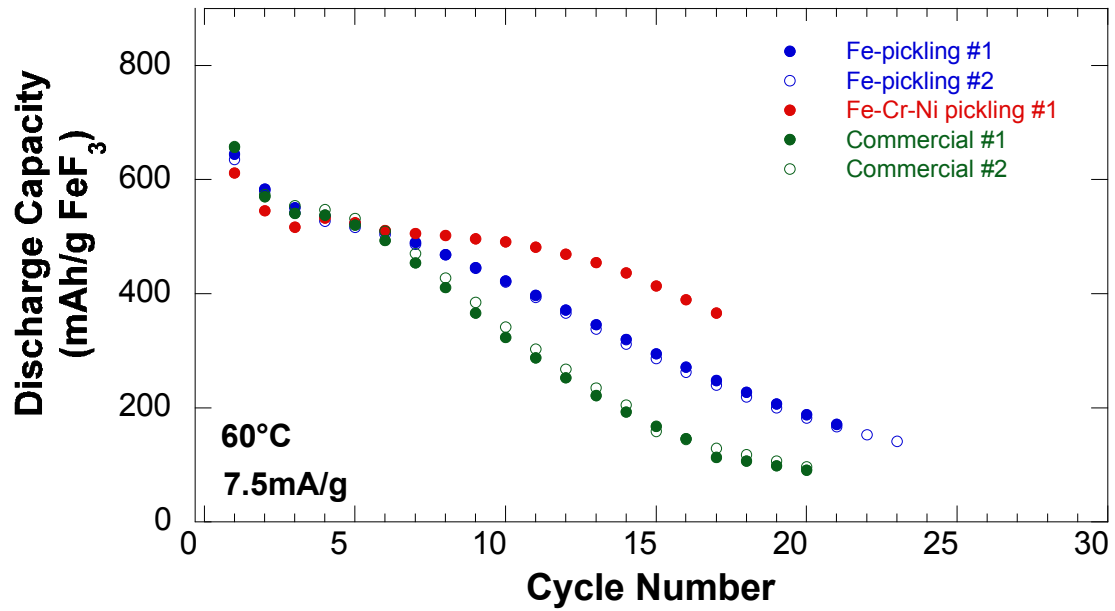


Figure 13- Discharge capacity (per gram of active FeF_3) versus cycle number of the samples synthesized from pickling liquors compared commercial FeF_3 performed at 60°C and 7.5 mA/g based on the weight of the nanocomposite.